

Supplementary Information

A facile self-templating synthesis of carbon framework with tailored hierarchical porosity for enhanced energy storage performance

Jie Yang^{1,2#}, Gaoran Li^{1,3#}, Meidan Cai¹, Pengju Pan¹, Zhoupeng Li¹, Yongzhong Bao^{1*}, Zhongwei Chen^{3*}

1. College of Chemical and Biological Engineering, Zhejiang University, Hangzhou 310027, China

2. Wanhua Chemical Co., Ltd. Yantai, China

3. Department of Chemical Engineering, Waterloo Institute for Nanotechnology, University of Waterloo, 200 University Avenue West, Waterloo, Ontario, N2L 3G1, Canada

* Correspondence to Prof. Yongzhong Bao, E-mail: yongzhongbao@zju.edu.cn; Prof. Zhongwei Chen, E-mail: zhwchen@uwaterloo.ca

Jie Yang and Gaoran Li contributed equally to this work.

Experimental

Chemicals

VDC (polymerization grade) was supplied by Juhua Group Co. (China) and distilled twice at an atmosphere of N₂. Methyl acrylate (MA) purchased from J&K Chemical Reagent Co. Ltd., was purified by vacuum distillation. The macro-RAFT agent, poly(acrylic acid)-*b*-polystyrene copolymer terminated with 2-(dodecylthiocarbonothioylthio)-2-methylpropionic acid group (PAA-*b*-PS-TTCA) was synthesized according to a previous method¹. 2,2'-Azobis[2-(2-imidazolin-2-yl)propane]dihydrochloride (VA044, >99%), sodium hydroxide (NaOH, >96%) and potassium hydroxide (KOH, >95%) were purchased from J&K Chemical Reagent Co. Ltd.. Polyvinylidene fluoride (PVDF, HSV900, Arkema Inc. France), elemental sulfur (Aladdin, China) and super P carbon (TIMCAL, Switzerland) were used as received.

*Preparation of PVDC-*b*-PS copolymers*

Ab initio emulsion copolymerization was used to synthesize the VDC random copolymer containing 10wt% MA (entitled as PVDC) by using VA044 as the initiator, and PAA-*b*-PS-TTCA as both the surfactant and chain transfer agent¹. PVDC-*b*-PS copolymers with different compositions (entitled as PVDC-*b*-PS_x, *x* means weight percent of PS in copolymer) were prepared by the seeded emulsion polymerization of styrene using PVDC as the seed and chain transfer agent.

Fabrication of HPCs

HPCs were prepared by the direct carbonization of PVDC-*b*-PS copolymer precursors. The carbonization was conducted at a heating rate of 10 °C/min under a N₂ flow of 200 ml·min⁻¹. In order to complete dehydrochlorination, PVDC-*b*-PS copolymers was first held at 200 °C and 300 °C for 1h, respectively. The samples were then heated to 900 °C at a heating rate of 5 °C/min and held for 4 h before cooling.

Materials characterization

Molecular weights of copolymers were characterized by dynamic gel permeation chromatography (GPC, Waters 1525/2414, USA) equipped with a Waters Styragel[®] column. THF was used as the eluent and PS samples with narrow molecular weight distributions were used as the standard. Thermogravimetric analysis (TGA) was conducted on a Perkin-Elmer Pyris1 TGA. The samples were heated to from 50 °C to

800 °C at a heating rate of 10 °C·min⁻¹ under a N₂ atmosphere. X-ray diffractometer (XRD, X'Pert PRO, PANalytical, Netherland) was used to investigate the crystal structure of the HPCs with Ni-filtered Cu K α radiation ($\lambda = 1.54056$). Raman spectroscopic analysis of prepared PVDC and HPCs was carried out with a JobinYvon HORIBA Raman spectrometer with 532nm He-Ne laser as the excitation source. The phase morphology of specimens was observed on a transmission electrical microscopy (TEM, JEM 1230, JEOL, Japan) operated at a voltage of 80 kV; The cast film samples were cryo-cut (ULTRACUT UC7, Leica, German); All the specimens were stained by OsO₄ vapor. The morphological changes of PVDC-*b*-PS copolymer films during thermal treatment examined on atomic force microscopy (AFM, Nanoscope IIIa MultiMode SPM, Veeco, USA) operated in the tapping mode. The samples were prepared by spin-coating the high concentration of PVDC-*b*-PS solution (50mg/ml in THF) on a silica plate for many times to simulate the bulk polymer and carbonizing the thick films at different temperature. The morphology of HPCs was observed by field emission scanning electron microscopy (SEM, CorlzeisD Utral55, German). The porous structure of each sample was analyzed by nitrogen adsorption analysis (Autosorb-1-C, Quantachrome, USA) at 77 K. The specific surface area and micropore volume were determined using the Brunauer-Emmett-Teller (BET) equation ². The pore size distribution was calculated from the absorption data using the nonlocal-density functional theory (NLDFT), assuming that the pores are slit/cylinder-shaped.

Electrochemical characterization

Supercapacitor

Electrodes based on HPCs were prepared by coating slurry containing HPCs and PVDF binder in mass ratio of 9:1 on commercial nickel foam. The coating area was 1 cm² and the mass loading was 1~2 mg cm⁻². Cyclic voltammetry (CV) and galvanostatic charge-discharge (GCD) data were collected by CHI660E electrochemical work station (Chinstruments, China) in a three-electrode system. Platinum wire and mercury-mercuric oxide electrode were used as counter electrode and reference electrode respectively. 6M KOH solution was used as electrolyte and the testing potential ranged from -0.7 to +0.1 V vs. Hg/HgO. Different scan rates and current densities were applied for CV and GCD test respectively to investigate the EDLC performances of electrodes

based on prepared HPCs. A long-term cycling test was also performed for HPC25 electrode at 2 A g⁻¹ density. All the tests were carried out under room temperature. Electrochemical characterization in symmetric two-electrode configuration was also performed for HPCs electrodes in CR2032 coin cell to further evaluate their capacitive performance.

From the charge-discharge curve, the specific capacitance (C_{spec}) of the electrodes was calculated using the following equation:

$$C_{spec} = \frac{I \times \Delta t}{\Delta V \times m} \quad (E1)$$

in which I is the discharge current, m is the electrode mass, Δt is the discharge time, and ΔV is the voltage range.

Li-S batteries

Sulfur/HPCs composites (S@HPCs) were prepared by thermal treatment for ball-milled mixture containing sulfur and HPCs in mass ratio of 7:3 at 155 °C for 4 h under N₂ atmosphere. Sulfur electrodes based on HPCs were prepared via a conventional slurry-casting method. The slurry contains HPCs@S, super P and PVDF in mass ratio of 7:2:1. The electrodes were obtained after casting the slurry on aluminum foil and vacuum dried at 60 °C for 12h. The electrochemical performances of the prepared sulfur electrodes were tested in CR2505 coin cells at room temperature using LAND battery cycler (China). Cells were assembled in Ar-filled glove box using metallic lithium wafer as counter electrode and Celgard 2325 membrane as separator respectively. The electrolyte contained 1M lithium bis(trifluoromethane sulfonyl) imide (LiTFSI) in a binary solvent of 1,3-dioxolane (DOL) and dimethoxyethane (DME) (1:1 in volume) with 1 wt% lithium nitrate (LiNO₃) as additive. The sulfur loading on electrode was 1.5~2 mg cm⁻². The electrolyte addition was 20 μL mg⁻¹_S. Current density and specific capacity were calculated based on the mass of S active material. The cyclic voltammetry and electrochemical impedance spectroscopy (EIS) study were recorded by CHI660E electrochemical work station (Chinstruments, China). The CV was tested in voltage range of 1.8-2.6 V vs. Li⁺/Li at a scan rate of 0.1 mV s⁻¹. The EIS was tested with amplitude of 5 mV in the frequency range of 0.01 Hz-100 kHz.

Table S1 Conditions of RAFT emulsion polymerization and structure parameters of PVDC and PVDC-*b*-PS copolymers ^a

Sample	$[M]_0/[CTA]_0$ ^b	Time (min)	Conversion (%)	$M_{n, GPC}$ ($\text{g}\cdot\text{mol}^{-1}$)	<i>PDI</i>
PVDC ¹	323	420	77	23000	1.49
PVDC-PS5	125	640	10	24100	1.52
PVDC-PS25	250	660	48	35500	1.70
PVDC-PS52	350	510	80	53200	1.80
PVDC-PS70	516	600	90	76300	1.60
PVDC-PS74	627	720	93	88800	1.66

^a: The content of chain transfer agent (CTA) is $2.9 \text{ mmol}\cdot\text{L}_{\text{aq}}^{-1}$ in reaction. For PVDC, it use PAA-*b*-PS-TTCA as CTA; For PVDC-*b*-PS, it use PVDC-TTCA as CTA. ^b: $[M]_0$ and $[CTA]_0$ are original concentration of monomer and chain transfer agent, respectively.

Table S2 Summary of the pore structure characteristics of the prepared HPCs *

Sample	S_{BET} ($\text{m}^2\cdot\text{g}^{-1}$)	V_{total} ($\text{cm}^3\cdot\text{g}^{-1}$)	V_{micro} ($\text{cm}^3\cdot\text{g}^{-1}$)	$V_{\text{micro}}/V_{\text{total}}$ (%)	D_{micro} (nm)	D_{aver} (nm)
PVDC	857.8	0.34	0.32	93.6	0.52	1.58
HPC5	927.8	0.78	0.33	41.8	0.63	3.35
HPC25	1239.7	1.43	0.42	29.4	0.60	4.72
HPC52	1160.1	1.66	0.40	23.9	0.59	5.73
HPC70	1225.6	1.86	0.43	23.2	0.59	6.10
HPC74	1197.3	1.95	0.43	21.9	0.59	6.51

*: S_{micro} and V_{micro} are calculated via t -plot method, D_{micro} are calculated via DFT method

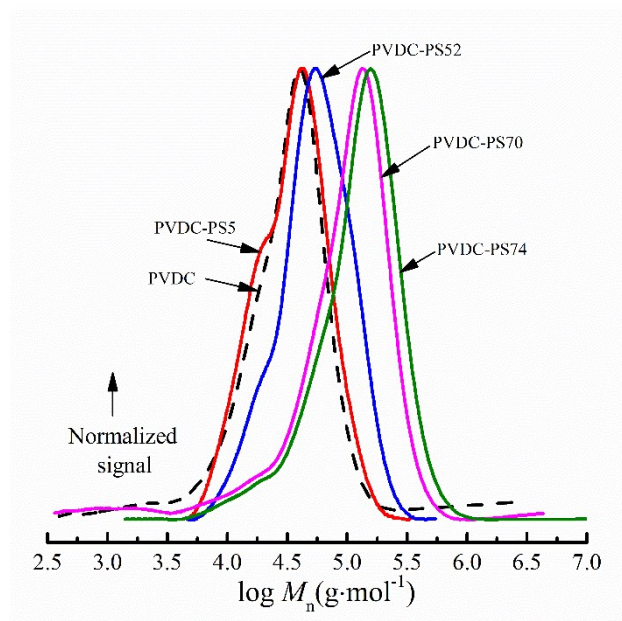


Fig. S1 GPC traces of seed emulsion polymerization of PVDC-*b*-PS copolymers

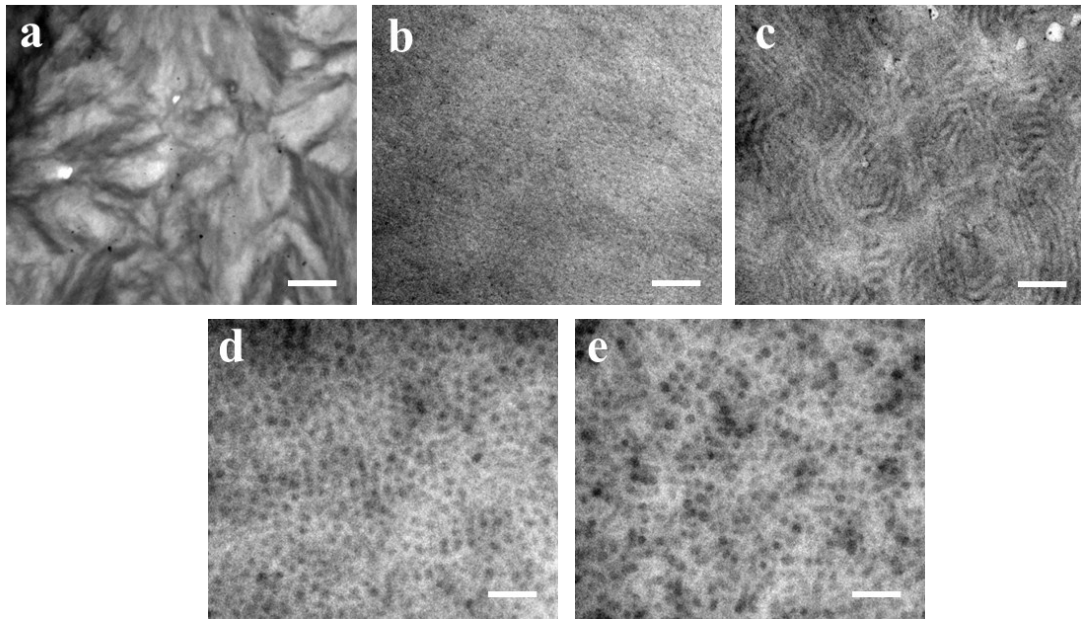


Fig. S2 TEM images of PVDC (a) and PVDC-*b*-PS copolymers(scale bar equals to 200 nm) (b) PVDC-PS5, (c) PVDC-PS25, (d) PVDC-PS52, (e) PVDC-PS74

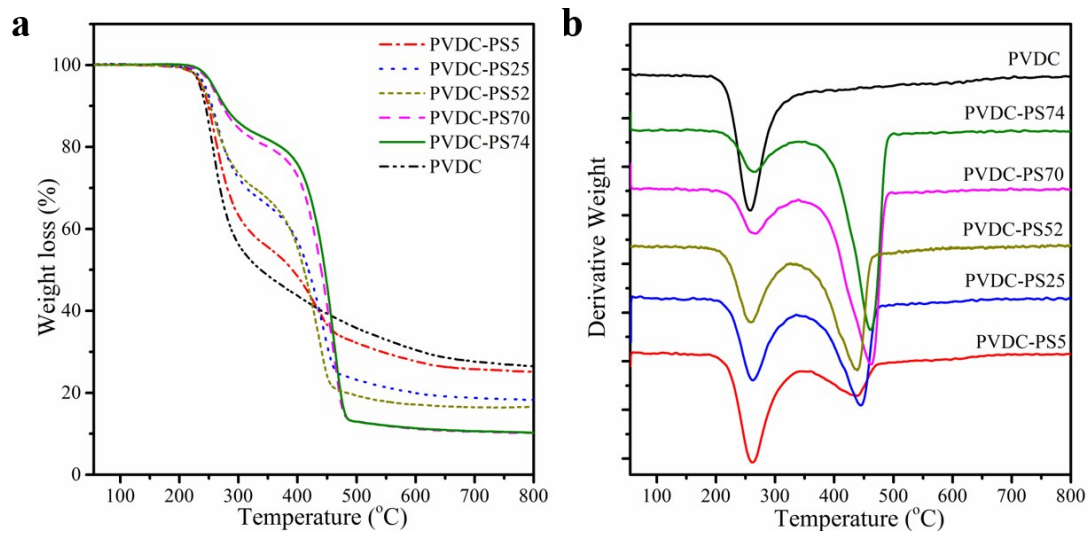


Fig. S3 TGA curves (a) and their derivative curves (b) of PVDC and PVDC-*b*-PS copolymer precursors for HPCs

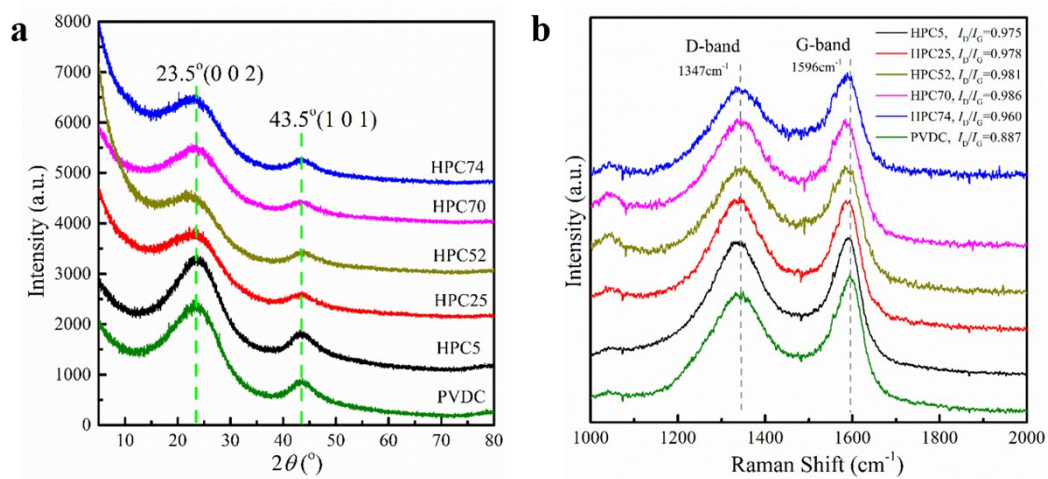


Fig. S4 (a) X-ray diffraction patterns and (b) Raman spectra of pure PVDC carbon and different HPCs.

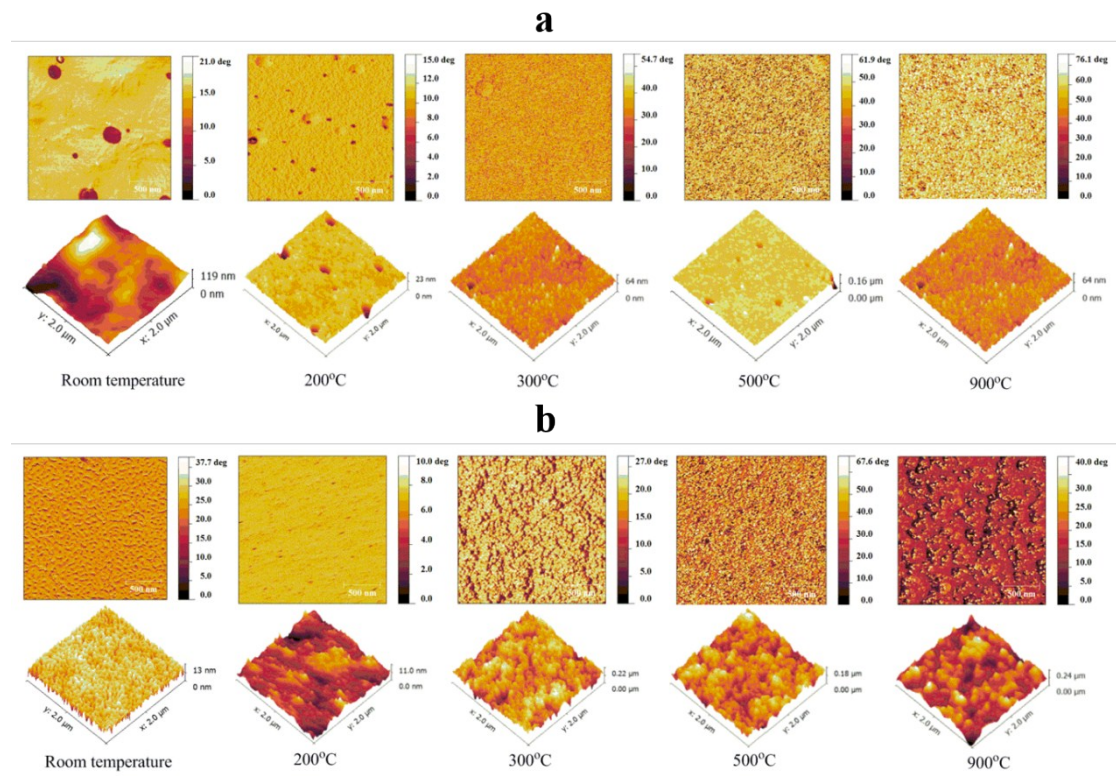


Fig. S5 AFM phase images (top) and height images (bottom) of PVDC-PS5 and its carbonized product films (a), and PVDC-PS74 and its carbonized product films (b) varied with thermal treatment temperature under N_2 .

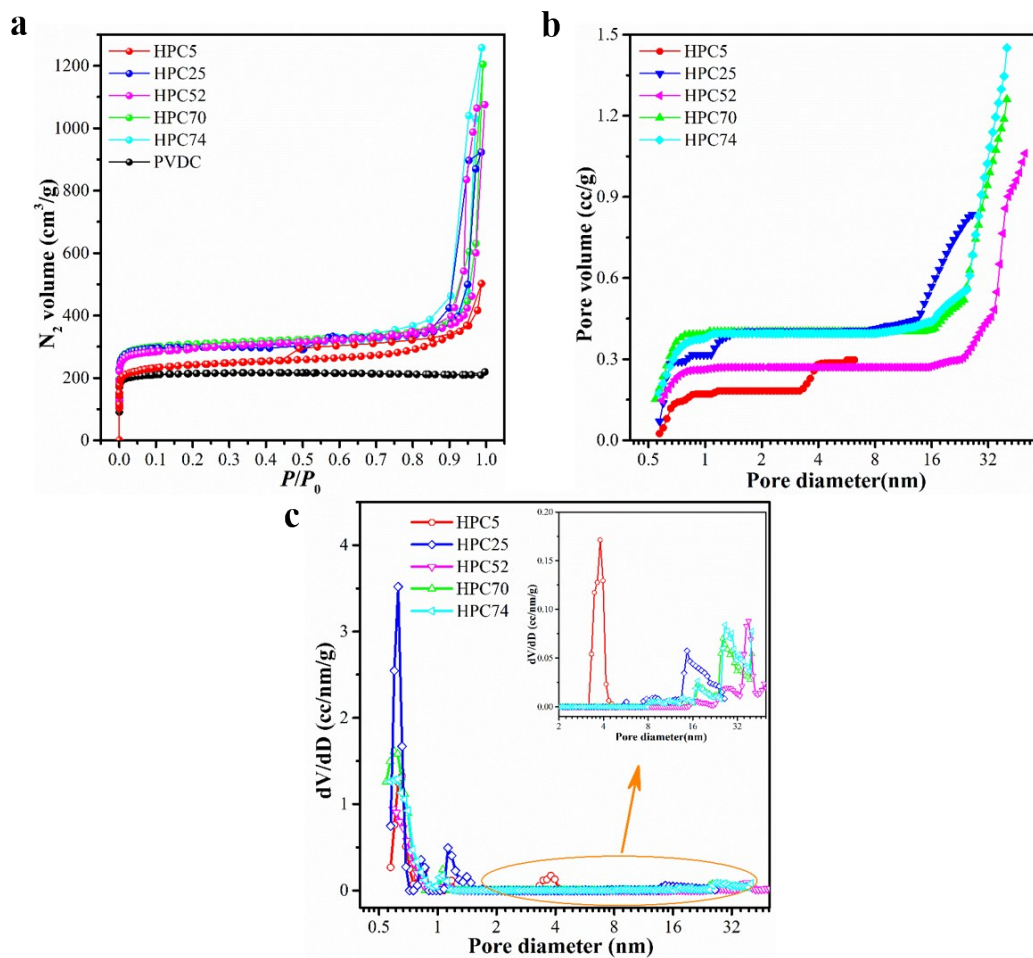


Fig. S6 (a) N₂ adsorption and desorption isotherms, (b) cumulative pore volume curves and (c) pore size distributions of HPCs. The inset in (c) shows the enlarged mesoporous distributions of HPCs.

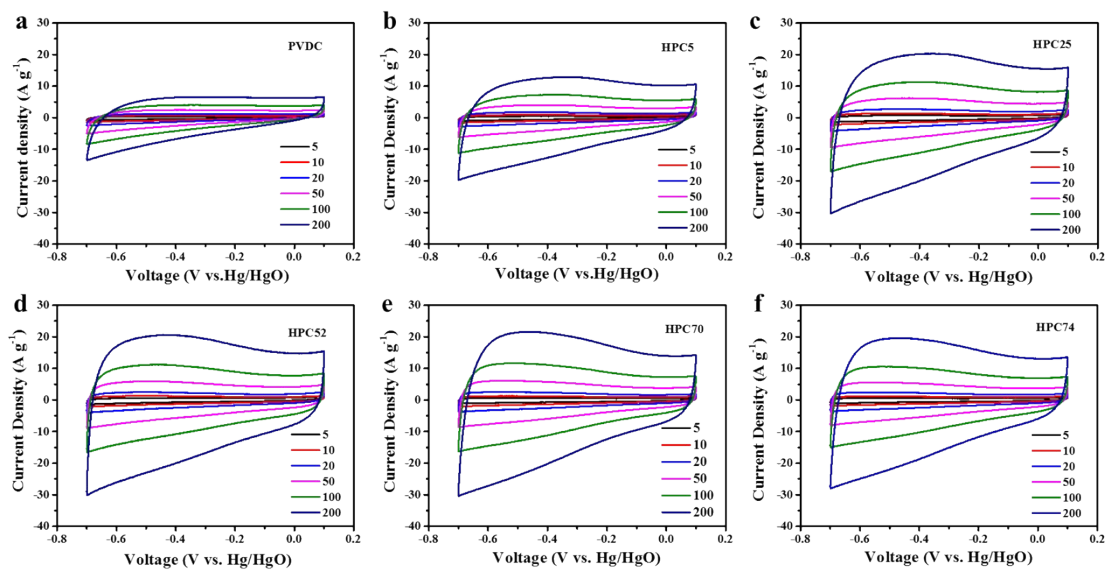


Fig. S7 CV curves of PVDC and HPCs electrodes at different scanning rates.

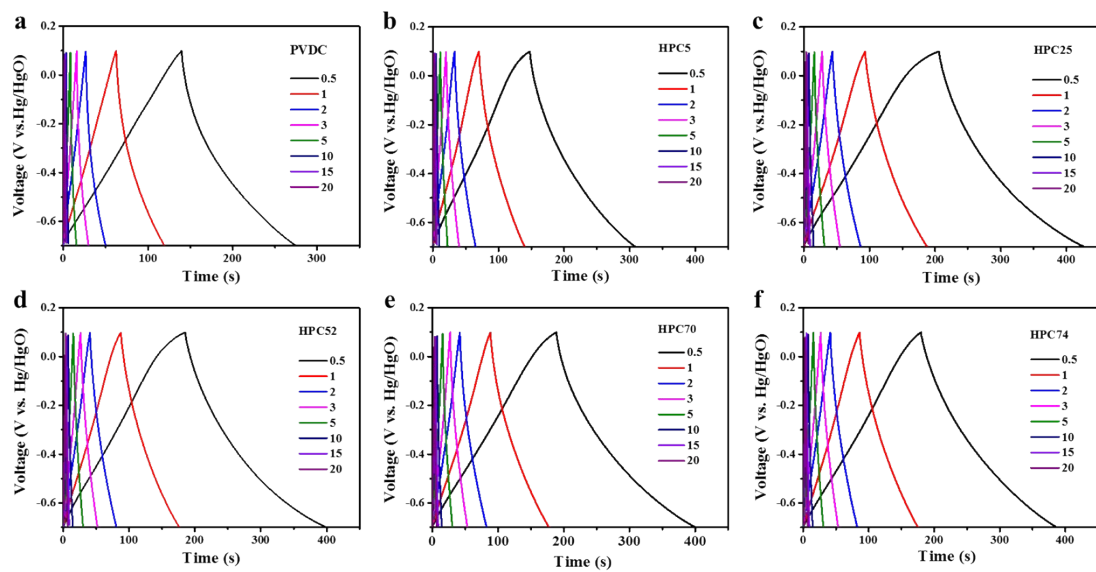


Fig. S8 GCD curves of PVDC and HPCs electrodes at different current densities of 0.5, 1.0, 2.0, 3.0, 5.0, 10, 15, 20 A g^{-1} .

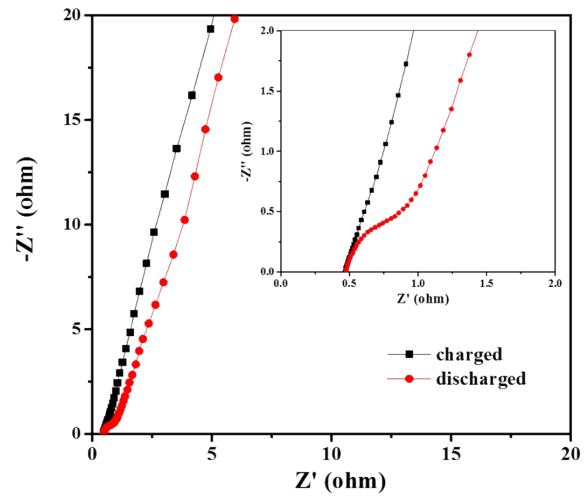


Fig. S9 EIS spectra of HPC74 electrode under charged and discharged states.

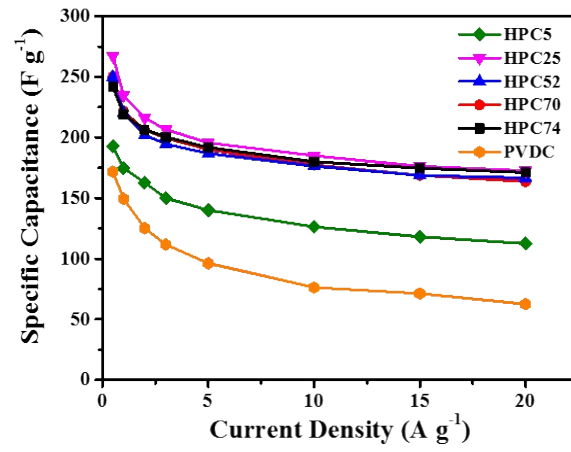


Fig. S10 Capacitances of HPCs electrode under varied current densities

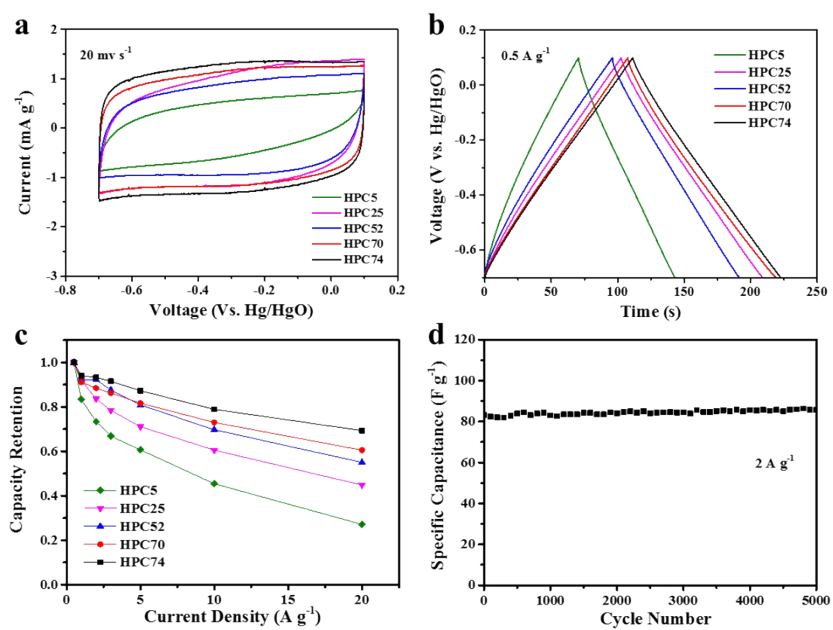


Fig. S11 Symmetric two-electrode characterization of HPCs. (a) CV curves at 20 mV s^{-1} , (b) GCD curves at 0.5 A g^{-1} , and rate capability of different HPC electrodes. (d) Long-term cycling of HPC74 electrode at 2 A g^{-1} .

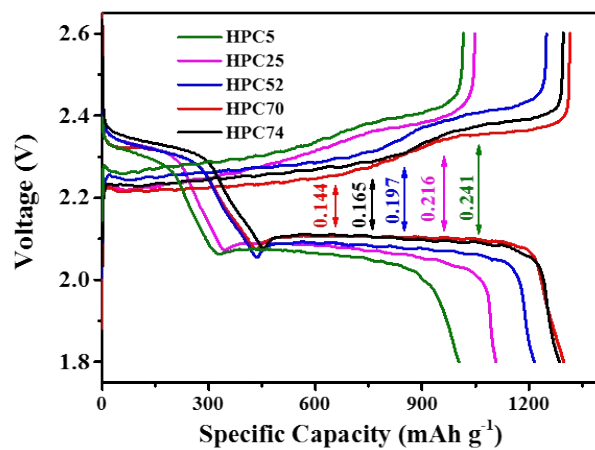


Fig. S12 Charge-discharge profiles and the polarization potential gaps of S@HPCs electrodes.

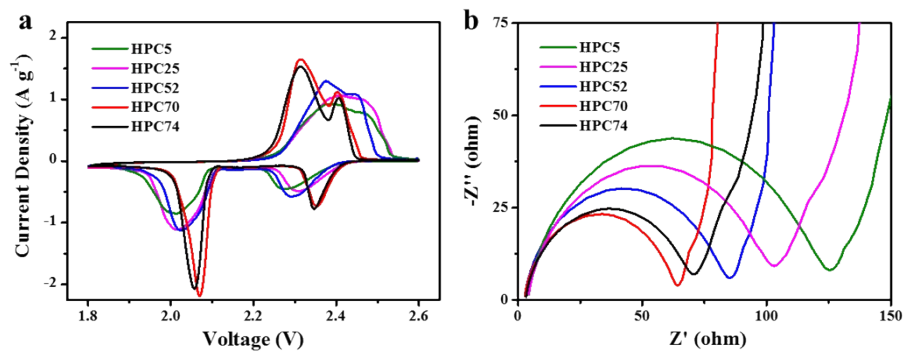


Fig. S13 (a) CV curves at 0.1 mV s^{-1} and (b) Nyquist plots of S@HPCs electrodes.

References

1. J. Yang, Y. Bao and P. Pan, *J APPL POLYM SCI*, 2014, **131**, 40391.
2. S. Brunauer, P. H. Emmett and E. Teller, *J AM CHEM SOC*, 1938, **60**, 309-319.